Label-Free Assay for Thermodynamic Analysis of Protein−Ligand Interactions: A Multivariate Strategy for Allosteric Ligand Screening†

Jennilee M. A. Gavina, Mohammad T. Mazhab-Jafari, Giuseppe Melacini, and Philip Britz-McKibbin*

Department of Chemistry, McMaster University, 1280 Main Street West, Hamilton, ON, Canada L8S 4M1

Received November 17, 2008; Revised Manuscript Received December 16, 2008

ABSTRACT: The binding of allosteric ligands to protein can induce changes to the holoprotein conformation, stability, and activity that have an impact on unfolding dynamics. Herein we report a label-free strategy for determining the dissociation constant of protein−ligand interactions over a wide dynamic range (>10^4, K_d from nano- to millimolar) using capillary electrophoresis that overcomes the constraints of an ideal two-state protein unfolding model. Multivariate analysis of thermodynamic parameters associated with holoprotein unfolding and ligand binding is demonstrated for the classification of cyclic nucleotide analogues that function as allosteric modulators of regulatory proteins, such as the exchange protein directly activated by cAMP (EPAC).

Successful identification of small molecule modulators of cellular activity is a critical step in modern drug discovery (*1*). To date, high-throughput screening methods have relied primarily on fluorescence and competitive radiolabel assays for ligand selection since binding affinity is related to drug potency (*2*). There is growing interest in the development of label-free strategies which are compatible with small amounts of impure protein samples and/or complex ligand mixtures, such as frontal affinity chromatography−electrospray ionization MS (*3*) and matrix-assisted laser desorption ionization MS (*4*). New methods that avoid protein immobilization, chemical labeling, and/or complicated off-line sample preparation while providing additional thermodynamic criteria for assessing high-affinity interactions are also desirable features for improving lead optimization of drug candidates (*5*). Herein, we describe a label-free strategy for determining the dissociation constant (K_d) of effector molecules from protein receptors over a wide dynamic range using dynamic ligand exchange−affinity capillary electrophoresis (DLE−ACE) (*6*), which is based on the relative conformational stability of different apo/holoprotein states upon unfolding (see the Supporting Information). A unique feature of DLE−ACE is the ability to electrokinetically generate different apo/holoprotein states directly in capillary using a femtomole protein sample with conventional UV detection (*7*) (see Scheme 1 of the Supporting Information). Access to multiple thermodynamic parameters associated with holoprotein unfolding and ligand binding can provide insight into the function of allosteric ligands that activate or inhibit the activity of regulatory protein involved in signal transduction (*8*).

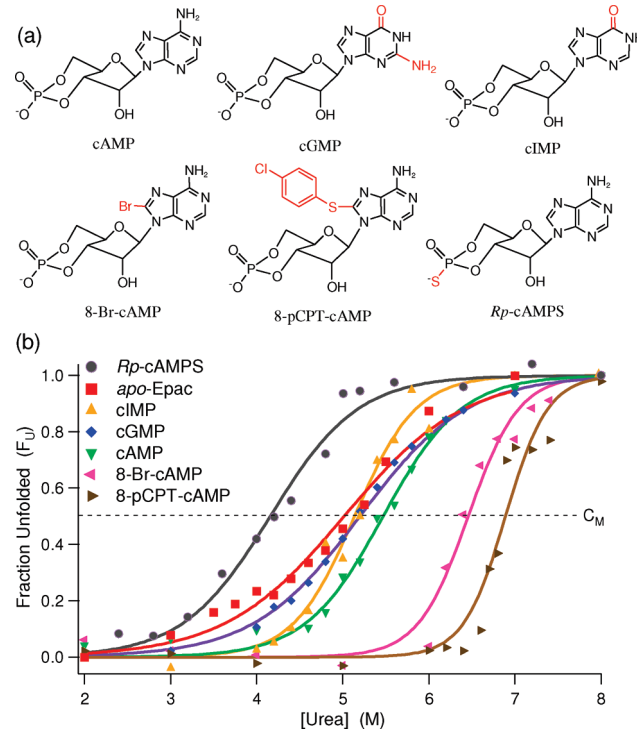

FIGURE 1: Impact of cNT binding on the conformational stability of EPAC upon urea denaturation by DLE−ACE, where (a) shows two-dimensional chemical structures of different cNT analogues and (b) compares apo/holoprotein unfolding curves based on the average viscocity-corrected apparent mobility of protein, $\nu\mu^{A}_{ep}$ (symbols; $n = 3$, CV < 5%) assuming an ideal two-state model, where C_M represents the midpoint for urea denaturation ($F_u = 0.5$).

The thermodynamics of EPAC (residues 149−318) binding to various cyclic nucleotide (cNT) analogues was examined as a model system in this work, which is a recently discovered cAMP-responsive guanine nucleotide exchange factor for the small GTP-binding proteins Rap1 and Rap2 (*9*). There is growing interest in the development of ligands that selectively target EPAC due to its altered expression in several chronic disorders, such as Alzheimer's disease (*10*). Figure 1 depicts the chemical structures of six cNT analogues (i.e., training set), as well as an overlay of protein unfolding curves derived from DLE−ACE experiments, which highlights the significant impact of ligand binding on holoprotein conformational stability. In general, cNTs that possess higher affinity for EPAC (e.g., 8-pCPT-cAMP) generate holo-EPAC−cNT complexes with intrinsic stability ($\Delta G°_U$) and

† We thank NSERC (to P.B.-M.) and CIHR (to G.M.) for financial support for this work. J.M.A.G. also acknowledges support from NSERC-CGS D.

* To whom correspondence should be addressed. Telephone: (905) 525-9140, ext. 22771. Fax: (905) 522-2509. E-mail: britz@mcmaster.ca.

10.1021/bi802121g CCC: $40.75
Published on Web 12/29/2008

Table 1: Relative Thermodynamic Parameters Associated with holo-EPAC−cNT Complex Unfolding and Ligand Binding Affinity

cNT[a]	$\Delta\Delta G°_U$[b] (kcal/mol)	Δm[b] (kcal mol^{-1} M^{-1})	ΔC_M[c] (M)	K_d[d] (μM)	K_d[e] (μM)
(R_p)-cAMPS	0.54	0.26	−0.58	305	340
cGMP	0.97	0.12	0.41	33	37
(S_p)-cAMPS	2.44	0.56	−0.10	28	34
cAMP	2.70	0.33	0.94	4.6	2.9
cIMP	4.52	0.83	0.13	12	10
8-Br-cAMP	8.72	1.12	1.70	0.23	0.36
8-pCPT−2′-*O*Me-cAMP[f]	11.4	1.94	0.79	0.13	0.41
8-pCPT−cAMP	16.9	2.20	2.10	0.051	0.045

[a] $\Delta G°_U$, m, and C_M values for apo-EPAC were 4.28 ± 0.12 kcal/mol, 0.90 ± 0.02 kcal mol^{-1} M^{-1}, and 4.75 ± 0.04 M, respectively. [b] Fitting error from protein unfolding curves; CV (±1σ), 2−12%. [c] $\Delta C_M = (\Delta G°_U/m)_{holo} - (\Delta G°_U/m)_{apo}$. [d] Predicted K_d of model cNTs using MLR calibration; CV (±1σ), 38−80%. [e] K_d from ref *11* using a competitive [^{3}H]cAMP radiolabel assay. [f] Rapid unfolding assay (<1 h) with limited data for K_d estimation. Note that (S_p)-cAMPS and 8-pCPT−2-OMe-cAMP were used for subsequent validation of the MLR model.

unfolding cooperativity (m) (i.e., slope of the unfolding transition region) greater than those of apo-EPAC. Stronger binding was also directly associated with an increase in the midpoint for urea denaturation (C_M). Interestingly, (R_p)-cAMPS was the only ligand that resulted in a major decrease in C_M relative to that of apo-EPAC despite its apparent greater $\Delta G°_U$. This anomaly suggests that EPAC binding to this phosphothiorate cNT analogue induces destabilization of the native protein conformation that is more susceptible to urea denaturation (*12*). Indeed, (R_p)-cAMPS has been reported to function as an allosteric inhibitor of EPAC activation, unlike its stereoisomer, (S_p)-cAMPS, that is an allosteric agonist (*13*). The higher $\Delta G°_U$ for the holo-EPAC−(R_p)-cAMPS complex relative to that of apo-EPAC is likely an artifact from extrapolation to zero urea concentration due to the differences in their m values (*14*).

The apparent dissociation constant (K_d) for protein−ligand interactions can be derived from protein unfolding experiments based on the relative free energy change ($\Delta\Delta G°_U$) measured between holo-EPAC−cNT and apo-EPAC states (see the Supporting Information). However, several caveats apply to ensure accurate determination of absolute K_d, which include equivalent m values for both apo- and holoprotein states undergoing a reversible two-state unfolding process without partially folded intermediates (*4, 15*). The latter assumptions can result in a significant bias in K_d determination when characterizing an allosteric protein such as EPAC, which requires multiple structural changes upon ligand binding to release self-inhibition of the catalytic region of the protein (*16*). Moreover, apo-EPAC has recently been shown to exist in dynamic equilibrium between active and inactive states in the absence of cAMP (*17*), which is consistent with an allosteric activation model in which ligand binding induces shifts in preexisting conformer populations (*8*). In this study, only $\Delta\Delta G°_U$ values for cGMP provided a reasonable estimate for a K_d of ≈20 μM (*11*) due to its similar m value with apo-EPAC, whereas a highly overestimated binding affinity was determined for all other cNT analogues when using apparent $\Delta\Delta G°_U$ values (see Table 1 of the Supporting Information). The magnitude of this bias was proportional to the difference in unfolding cooperativity between apo- and holo-EPAC−cNT states (Δm). The large increase in Δm values measured for most holo-EPAC−cNT

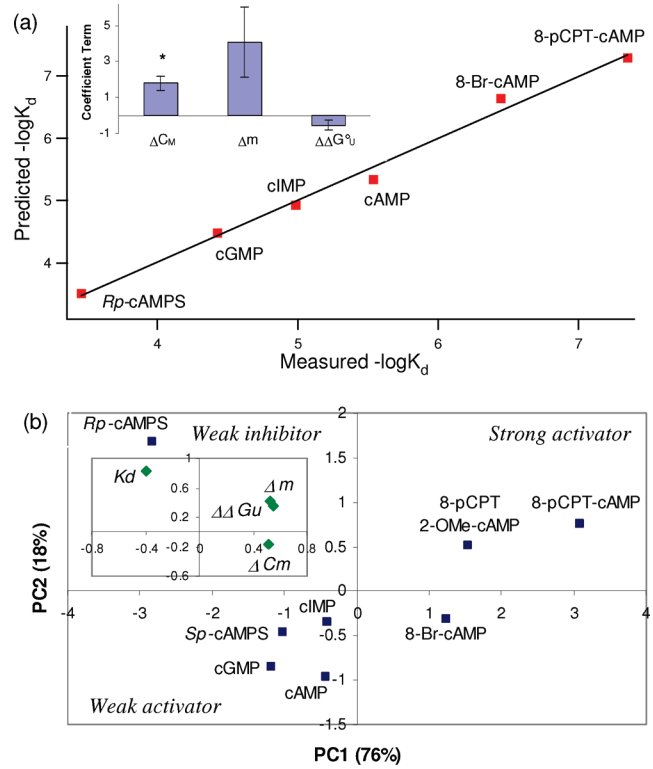

FIGURE 2: (a) Linear correlation plot ($y = 0.990x + 0.049$; $R^2 = 0.9954$) between predicted −log K_d values derived from holo-EPAC−cNT complex unfolding studies using DLE−ACE and measured −log K_d values of EPAC−cNT complex binding by a competitive radiolabel assay (*11*). The inset graph shows that ΔC_M was the most significant thermodynamic variable (*P < 0.05) directly correlated with higher EPAC−cNT binding affinity, unlike $\Delta\Delta G°_U$ when using MLR, where error bars represent ±1σ. (b) Two-dimensional scores plot using principal component analysis (PCA) for classifying different cNTs based on multiple thermodynamic criteria associated with holo-EPAC−cNT unfolding and binding for prediction of allosteric ligand function, where the inset depicts a loading plot that highlights the contribution of each thermodynamic variable on cNT coordinates within the scores plot.

complexes relative to apo-EPAC can be attributed to their reduction in solvent accessible surface area (*18*) and/or the lack of partially unfolded intermediates in the transition region (*14*) that is suggestive of an increasingly homogeneous conformer population. In cases where Δm values for different holoprotein states are similar in magnitude yet different from that of apo-EPAC, relative K_d values can be determined directly from unfolding parameters (*6*) without bias caused by extrapolation of $\Delta G°_U$ to native conditions.

Table 1 summarizes the three major thermodynamic parameters determined for unfolding of the holo-EPAC−cNT complex relative to apo-EPAC. We observed that there was a significant linear correlation ($R^2 = 0.9474$) between ΔC_M parameters from unfolding studies in this work and −log K_d reported using a competitive [^{3}H]cAMP binding assay (*11*). However, multiple linear regression (MLR) using all three thermodynamic variables provided improved correlation ($R^2 = 0.9910$) and greater predictive accuracy for K_d over a 10^4-fold dynamic range (K_d from nano- to millimolar) as shown in Figure 2a. Since ΔC_M is defined as the relative ratio of $(\Delta G°_U/m)_{holo} - (\Delta G°_U/m)_{apo}$, it serves as a useful parameter for normalizing changes in apparent $\Delta G°_U$ when different holo-EPAC−cNT states are compared (see the Supporting Information). The inset of Figure 2a confirms

that ΔC_M is statistically the most significant ($P = 0.05$) thermodynamic variable positively correlated with higher binding affinity. Overall, the average relative error in the absolute K_d values was ~16% when results were compared with a validated radiolabel assay (*11*). Two additional cNT analogues (i.e., test set) were also examined to further validate the predictive capability of the model (Figure 2 of the Supporting Information). Table 1 shows that (S_p)-cAMPS was observed to have $\Delta\Delta G°_U$ and Δm terms similar to those of cAMP but with a 6-fold lower affinity ($K_d \approx 28$ μM), which is consistent with its function as a weak EPAC activator (*11*). Recent studies have demonstrated that the 8-pCPT−2-OMe-cAMP species has an ~10^3-fold increase in target selectivity for EPAC relative to cAMP-dependent protein kinase A with superagonist activity (*11, 13*). In this case, a limited unfolding study for the holo-EPAC−8-pCPT−2-OMe-cAMP complex was also performed (see the Supporting Information) to demonstrate the feasibility for rapid estimation of K_d by DLE−ACE. Table 1 confirms that improving EPAC selectivity via 2-OMe ribose modification of 8-pCPT-cAMP is associated with a decrease in its binding affinity.

There is growing recognition that small globular proteins can often undergo multistate unfolding transitions despite being adequately described by an ideal two-state model in the absence of detectable partially folded intermediates (*14*). In this work, we have demonstrated that nonideality can be revealed by the disparity in apo/holoprotein unfolding cooperativity as inferred by significant differences in Δm, which hampers accurate determination of K_d directly from $\Delta\Delta G°_U$ values. Figure 2b summarizes the results from Table 1 using a two-dimensional scores plot from principal component analysis (PCA), which was applied to compare eight different cNT analogues on the basis of their four different thermodynamic variables associated with EPAC−cNT interactions, namely, ΔC_M, Δm, $\Delta\Delta G°_U$, and K_d (see the Supporting Information). It is evident that three major groups of allosteric ligands can be classified on this multivariate thermodynamic map, which provides insight into their putative mechanism of allosteric activation. For instance, (R_p)-cAMPS and the 8-modified cNT analogues represent two distinct classes of ligands for EPAC relative to cAMP, which is consistent with their reported activity as a weak antagonist and strong agonists, respectively (*13*). In contrast, (S_p)-cAMPS, cGMP, and cIMP appear as a group to function more like native cAMP, although cGMP and cIMP have been shown to behave as weak partial agonists of EPAC activation (*11*). Improved prediction of allosteric ligand function may be realized when using a full-length protein that undergoes global conformational changes upon ligand binding, unlike the truncated protein construct used in this study.

Ligands that target allosteric sites of a protein offer promising therapeutic benefits compared to traditional orthosteric drug design (*19*). However, caution is needed when comparing equilibrium unfolding studies involving a regulatory protein and different allosteric ligands since differences in Δm contribute to bias in $\Delta\Delta G°_U$ and K_d values. Our studies suggest that Δm is a parameter related to an overall increase in the homogeneity and ordering of holoprotein conformation(s) relative to the apo state, whereas ΔC_M is associated with the extent of ligand-induced stabilization or destabilization that can be quantitatively related to K_d via multivariate calibration. Future work will explore multivariate thermodynamic maps for improved selection of novel allosteric drugs by DLE−ACE, such as chemical chaperones (*20*) that are relevant in enzyme enhancement therapy for inborn errors of metabolism based on ligand-induced conformational stabilization of misfolded proteins.

SUPPORTING INFORMATION AVAILABLE

Details of experimental procedures, unfolding experiments, and data processing. This material is available free of charge via the Internet at http://pubs.acs.org.

REFERENCES

1. Bleicher, K. H., Böhm, H.-J., Müller, K., and Alanine, A. I. (2003) *Nat. Rev. Drug Discovery 2*, 369–378.
2. Hertzberg, R. P., and Pope, A. J. (2000) *Curr. Opin. Chem. Biol. 4*, 445–451.
3. Ng, E. S., Chen, N. W., Lewis, D. F., Hindsgaul, O., and Schriemer, D. C. (2007) *Nat. Protoc. 2*, 1907–1917.
4. Tang, L., Hopper, E. D., Tong, Y., Sadowsky, J. D., Peterson, K. J., Gellman, S. H., and Fitzgerald, M. C. (2007) *Anal. Chem. 79*, 5869–5877.
5. Ruben, A. J., Kiso, Y., and Freire, E. (2006) *Chem. Biol. Drug Res. 67*, 2–4.
6. Seguí-Lines, G., Gavina, J. M. A., D'Amaral, J., and Britz-McKibbin, P. (2007) *Analyst 132*, 741–744.
7. Gavina, J. M. A., Das, R., and Britz-McKibbin, P. (2006) *Electrophoresis 27*, 4196–4204.
8. Changeux, J.-P., and Edelstein, S. J. (2005) *Science 308*, 1424–1428.
9. de Rooij, J., Zwartkruis, F. J. T., Verheijen, M. H. G., Cool, R. H., Nijman, S. M. B., Wittinghofer, A., and Bos, J. L. (1998) *Nature 396*, 474–477.
10. McPhee, I., Gibson, L. C. D., Kewney, J., Darroch, C., Stevens, P. A., Spinks, D., Cooreman, A., and MacKenzie, S. J. (2005) *Biochem. Soc. Trans. 33*, 1330–1332.
11. Christensen, A. E., Selheim, F., de Rooij, J., Dremier, S., Schwede, F., Dao, K. K., Martinez, A., Maenhaut, C., Bos, J. L., Genieser, H. G., and Døskeland, S. O. (2003) *J. Biol. Chem. 278*, 35394–35402.
12. Cimmperman, P., Baranauskiene, L., Jachimoviciute, S., Jachno, J., Torresan, J., Michailoviene, V., Matuliene, J., Sereikaite, J., Bumelis, V., and Matulis, D. (2008) *Biophys. J. 95*, 3222–3231.
13. Rehmann, H., Schwede, F., Døskeland, S. O., Wittinghofer, A., and Bos, J. L. (2003) *J. Biol. Chem. 278*, 38548–38556.
14. Mayne, L., and Englander, S. W. (2000) *Protein Sci. 9*, 1873–1877.
15. Powell, K. D., and Fitzgerald, M. C. (2003) *Biochemistry 42*, 4962–4970.
16. Das, R., Mazhab-Jafari, M. T., Chowdhury, S., SilDas, S., Selvaratnam, R., and Melacini, G. (2008) *J. Biol. Chem. 283*, 19691–19703.
17. Harper, S. M., Wienk, H., Wechselberger, R. W., Bos, J. L., Boelens, R., and Rehmann, H. (2008) *J. Biol. Chem. 283*, 6501–6508.
18. Myers, J. K., Pace, C. N., and Scholtz, J. M. (1995) *Protein Sci. 4*, 2138–2148.
19. Christopoulos, A. (2002) *Nat. Rev. Drug Discovery 1*, 198–210.
20. Tropak, M. B., and Mahuran, D. (2007) *FEBS J. 274*, 4951–4961.

BI802121G